Bifunctional Magnetic Luminescent Particles Based on Iron Oxide Nanoparticles Grafted with a Europium Silylated Bypiridine Tris(β-diketonate) Complex

Robson R. Silva,*[a] Adriana P. Duarte,[b] Rafael M. Sábio,[a] José M. A. Caiut,[c] Marie Gressier,[d] Marie-Joëlle Menu,[d] Adolfo Franco Jr,[e] and Sidney J. L. Ribeiro[a]

A new highly magnetic-luminescent nanocomposites has been synthesized by grafting luminescent europium complex comprising tris(b-diketone) and bypridine ligand modified with a silylil function group (Eu[$(TTA)_3$(Bpy-Si)] complex) on the surface of superparamagnetic iron oxide nanoparticles with 11 nm in size coated with a thin silica outer layer. The γ-Fe_2O_3/SiO_2 nanoparticles were fully characterized by ATR-FTIR, FE-SEM, HR-TEM and magnetic measurements to confirm the structure of nanocomposite and the superparamagnetic behavior. Grafting with europium silylated bypiridine tris(β-diketonate) complex on nanoparticles surface was achieved by covalent bonding through triethoxysilyl groups which allows high concentration of the luminescent species. The resulting nanocomposite display superparamagnetic profile and the indirect excitation in the ultraviolet region outcomes high red luminescence intensity (at 613 nm) with narrow characteristic emission lines of Eu (III) and emission lifetime in the millisecond range. The nanocomposite is potentially useful for applications as biolabelling, imaging, bio-separation and bioassays.

Introduction

Grafting of optically active components at the surface of iron oxide magnetic nanoparticles has triggered great interest in the design of functional materials for medical diagnosis such as nano-bio-labelling and dual magnetic-optical imaging. Besides low toxicity and good biocompatibility, iron oxide nanoparticles show high coercivity, low Curie temperature, high magnetic susceptibility and, specially, they can display superparamagnetic behavior at room temperature. Owing to these features, iron oxide nanoparticles have been widely exploited in the development of contrast agents for magnetic resonance imaging and thermoacoustic tomography.[1,2]

Recently, significant efforts have been devoted towards the association of lanthanides (Ln) as luminophors with superparamagnetic iron oxide (SPIO) nanoparticles due to their unique optical properties such as narrow excitation and emission bands from ultraviolet to near-infrared region and relatively high emission quantum yield.[3–6] Remarkably, Ln luminophors provide long lifetimes (i.e. microseconds to milliseconds) enabling temporal selectivity based upon discrete signal detection without background fluorescence. Beyond the aesthetic appeal, long fluorescence lifetime of Ln luminophors combined with MRI contrasting properties delivered by SPIO nanoparticles are exciting features for the design of opto-magnetic probes for biological imaging in diagnosis.[7]

However, two main issues should be taking into account in the association of SPIO and Ln luminophors: i) Ln ions exhibit low molar absorption coefficient and, consequently, direct excitation rarely yields strong luminescence. Usually, this issue is overcome by complexing organic ligands (chromophores) to Ln ions, that absorb light and transfer energy to excited states of Ln ions which, finally, emit light with large Stokes-shifted fluorescence. ii) iron oxide is a well-known strong luminescence quencher. In the case of SPIO nanoparticles, the quenching of luminescence is mostly suppressed by covering their surface with a non-quenching layer.[8] So far, silica (SiO_2) is the most investigated inorganic layer for the immobilization of Ln complexes on SPIO nanoparticles.[9–13] Beyond that, the coating of SPIO nanoparticles with SiO_2 layer also enhances their chemical reactivity for post functionalization and improves their colloidal stability.[14] Two main strategies have been used for immobilization of Ln complexes onto the SPIO nanoparticles

[a] *Dr. R. R. Silva, Dr. R. M. Sábio, Prof. Dr. S. J. L. Ribeiro*
Institute of Chemistry
São Paulo State University UNESP
CP 355, Araraquara SP, 14801 970, Brazil
E mail: robsilva31@iq.unesp.br
[b] *Prof. Dr. A. P. Duarte*
Institute of Chemistry
Federal University of Mato Grosso do Sul
Campo Grande MS, 79070 900, Brazil
[c] *Prof. Dr. J. M. A. Caiut*
Departamento de Química
Faculdade de Filosofia, Ciências e Letras de Ribeirão Preto
Universidade de São Paulo
Ribeirão Preto SP, 14040 901, Brazil
[d] *Dr. M. Gressier, Prof. Dr. M. J. Menu*
Centre Interuniversitaire de Recherche et d'Ingénierie des Matériaux
Université de Toulouse, UPS CNRS 5085
118 route de Narbonne, 31062 Toulouse Cedex 9, France
[e] *Prof. Dr. A. Franco Jr*
Institute of Physics
Federal University of Goiás
Goiânia GO, 74690 900, Brazil

Supporting information for this article is available on the WWW under http://dx.doi.org/10.1002/slct.201601203

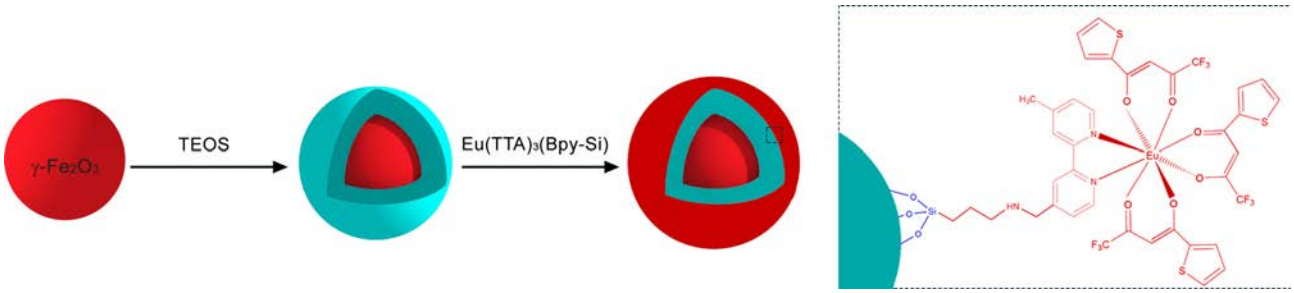

Figure 1. Representation of the synthesis of magnetic luminescent γ Fe_2O_3@[$Eu(TTA)_3$ (Bpy Si)].

coated with a SiO_2 shell: 1) a magnetic core is coated with Ln complex embedded in a SiO_2 shell.[15–17] This strategy delivers inhomogeneous distribution of the Ln complex which leads to clustering and hence the increase of the number of luminescent quenchers. Additionally, Ln complexes may be eventually leached from the silica shell due to weak interaction between luminophors and host layer which outcomes very low concentration of Ln complexes in the luminescent nanocomposite; 2) a magnetic core is initially coated with a SiO_2 shell and then grafted with silylated bridging ligands from Ln complex.[18,19] Remarkably, this last strategy prevents lixiviation processes and increases the luminophor concentration in the nanocomposite.

Many efforts have been dedicated to design of suitable silylated ligands required for efficient indirect excitation on Ln complexes. Silylated Tb^{III} complexes based on quinolones[20] and benzoate[21] ligands have been grafted at the surface of Fe_3O_4@SiO_2 core-shell nanoparticles. Feng and co-workers[22] have investigated the immobilization of Ln β-diketonates complexes onto Fe_3O_4@SiO_2 mesoporous particle surface by covalently grafting a silylated 1,10-phenanthroline as a second complex ligand. Luminescent complexes of Ln tris (dibenzylketonate) (5-[N, N-bis 3 - (triethoxysilil) propyl] ureil-1,10-phenanthroline (Ln=Yb^{III}, Nd^{III})[23] were grafted onto mesoporous silica shell containing Fe_3O_4 nanoparticles for controlled drug application and optical imaging in the near infrared (NIR) region. In previously studies, Menu and co-workers investigated the introduction of silylating groups in dipyridine[24] and β -diketonates[25,26] molecules in order to prepare silylated Eu^{III} complexes. Recently, some of us investigated the covalent bonding of [Eu(2-thenoyl-trifluoroacetone)$_3$-(4-methyl-4′-(methylaminopropylalkoxysilyl)-2,2′-dipyridine] named as [$Eu(TTA)_3$ (Bpy-Si)] inside uniform Stöber silica nanoparticles and spray-pyrolysis derived mesoporous silica particles.[27] This methodology allowed achieving luminescent silica nanoparticles with strong luminescence, high grafting ratios besides overcoming the release of chelate and tendency to agglomeration. Therefore, the luminescent nanohybrids were successfully applied as luminescent labels for bioimaging of bacteria biofilms.[27] Herein, we extended the incorporation of [$Eu(TTA)_3$(Bpy-Si)] complex to the surface of magnetic iron oxide nanoparticles covered with a thin silica layer. The schematic representation of the synthesis of γ-Fe_2O_3@[$Eu(TTA)_3$(Bpy-Si)] is displayed in Figure 1.

Results and Discussion

A description of the synthesis of luminescent [$Eu(TTA)_3$(Bpy-Si)] complex was previously reported by some of us elsewhere.[27] Typically, an aqueous suspension of γ-Fe_2O_3 nanoparticles was obtained by precipitation of aqueous Fe^{II} and Fe^{III} chloride solutions in ammonia solution followed by oxidation with diluted nitric acid under ambient air at 90 °C. The outcome relies to the presence of agglomerates containing individual iron oxide particles exhibiting nearly spherical shape and average size of 11 nm as displayed by TEM images of Figure 2, A and B. The diffraction rings at (200), (311), (400), (511), (422), (440) highlighted in selected-area electron diffraction and the peaks from X-ray diffraction pattern of γ-Fe_2O_3 nanoparticles showed in Figure 2, C and D respectively, are assigned to spinel face-centered cubic structure of iron oxide (JCPDS 39–1346). The dispersion of theses nanoparticles stands for an acid electrostatically stabilized aqueous ferrofluid displaying a zeta potential of +41 mV and low polydispersion index of 16.1 % at pH ~3.5. As expected from the DLVO theory, electrostatically stabilized ferrofluid faces severe particle agglomeration with the increase of pH and/or ionic strength. The isoeletric point (IEP) of acid ferrofluid corresponded to pH of 6.3, which was consistent with the IEP observed for pristine iron oxide surface. It is worth to taking into account that eventual agglomeration would be expected if the silica coating procedure using Stöber method is conducted directly with bare γ-Fe_2O_3 nanoparticles since such approach deals with the hydrolyzes and condensation of silica precursors under alkaline solution (pH >10). Therefore, γ-Fe_2O_3 nanoparticles were further modified with citric acid prior the silica coating procedure in order to prevent the formation of larger aggregates or the occurrence of undesirable phase transformations such as the formation of iron hydroxides. The colloidal stability of citrate-modified γ-Fe_2O_3 in alkaline solution is assured by partial ionization of carboxylate groups.

The functionalization of bare γ-Fe_2O_3 nanoparticles with citrate molecules was evaluated by assessing Fourier Transform Infrared Spectroscopy (FTIR). The purified citrate-modified γ-Fe_2O_3 nanoparticles display a pronounced doublet band assigned to υ_s(C=O) and υ_a(C=O) at 1589 cm^{-1} and 1400 cm^{-1}, respectively, whereas the doublet band at 583 cm^{-1} and 684 cm^{-1} are attributed to ν(Fe O) stretching mode of iron oxide in the FTIR spectrum showed in Figure 3.

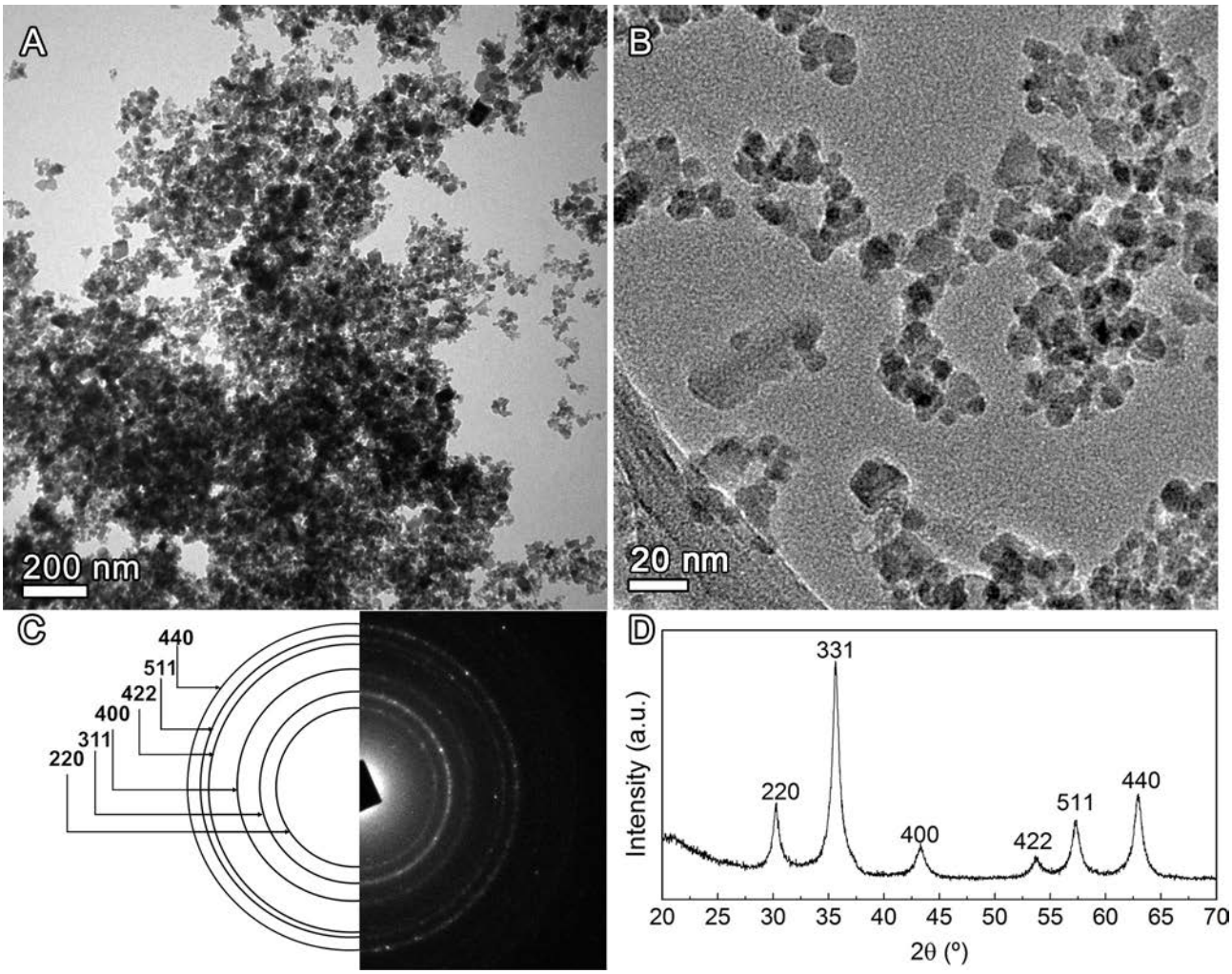

Figure 2. Representation of the synthesis of magnetic luminescent γ Fe_2O_3@[$Eu(TTA)_3$ (Bpy Si)] (A) and (B) TEM images, C) Selected area eletron diffraction and (D) X ray diffraction of pristine γ Fe_2O_3 nanoparticles.

Silica coating was achieved through a modified Stöber reaction. Citrate-modified γ-Fe_2O_3 nanoparticles served as nucleation seeds for further growth of silica layer. An ethanolic solution of tetraethylorthosilicate (TEOS) was slowly placed on an alkaline suspension of citrate-modified γ-Fe_2O_3 nanoparticles under vigorous stirring. Transmission Electron Microscopy (TEM) image of γ-Fe_2O_3@[Eu $(TTA)_3$(Bpy-Si)] nanoparticles displays the presence of agglomeration as shown in Figure 4 A. The High-Resultion Transmission Electron Microscopy (HRTEM) inset image shown in Figure 4B was recorded from the edge of a particle cluster. The lattice image and electron diffraction corresponds to the interplanar distance of γ-Fe_2O_3 (004) with d (004) = 0.29 nm. The HRTEM image also displays an outer and amorphous thin layer of silica (~ 3 nm average) coating the edge of nanoparticles.

Furthermore, the FTIR spectrum of resulting γ-Fe_2O_3/SiO_2 nanoparticles in Figure 5 displays intense bands at 1094 cm^{-1} and a shoulder at 956 cm^{-1} which are attributed to ν_a(Si O Si) and ν_s(Si-OH), respectively indicating incomplete condensation of silica network at γ-Fe_2O_3 nanoparticles surface. After SiO_2 coating, the IEP of γ-Fe_2O_3/SiO_2 nanoparticles decreased to pH ~ 2, resembling the IEP expected for amorphous silica surface. Benefiting from the SiO_2 coating, free Si-OH groups on the surface of γ-Fe_2O_3/SiO_2 particles rely on available anchorage sites for grafting of silylated Eu^{III} complex.

The grafting of [[$Eu(TTA)_3$(Bpy-Si)] complex was undertaken by mixing ethanolic suspensions of γ-Fe_2O_3/SiO_2 nanoparticles and [$Eu(TTA)_3$(Bpy-Si)] complex at room temperature. The silylated Eu complex is considered to be evenly distributed over the silica network surface. After several cycles of washing, the FTIR spectrum of γ-Fe_2O_3[$Eu(TTA)_3$(Bpy-Si)] particles shows additional bands at 1600 and 1614 cm^{-1} assigned to different ν(C═O) of diketone together with a narrow band at 1413 cm^{-1} attributed to the thenoyl moiety, conceiving the signature of the silylated Eu complex as displayed in the Figure 5 . The bands at 1538 and 1557 cm^{-1} are attributed to ν(C═C) and ν(C═N) modes of bypiridine ring. It is worth to pointing up that the FTIR spectrum of grafted silylated Eu complex also shows broad bands in the 1000–950 cm^{-1} region assigned to Si O Si and Si-OH vibrational modes.

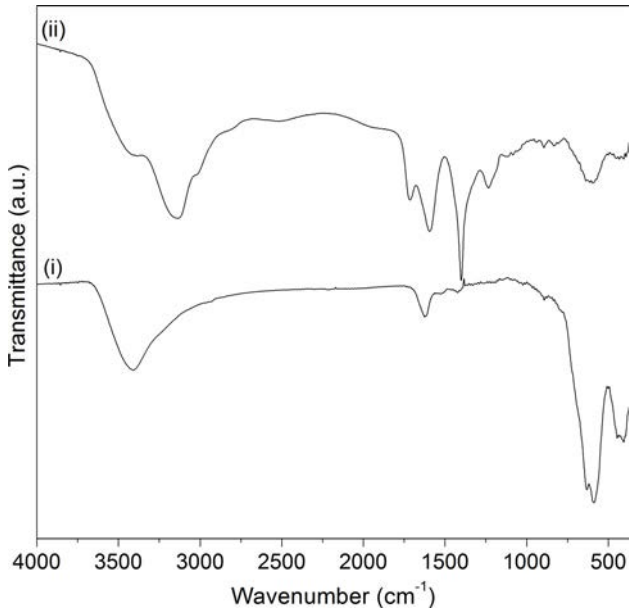

Figure 3. Fourier transform infrared vibrational spectra of (i) pristine γ Fe_2O_3 particles (ii) γ Fe_2O_3 particles functionalized with citric acid.

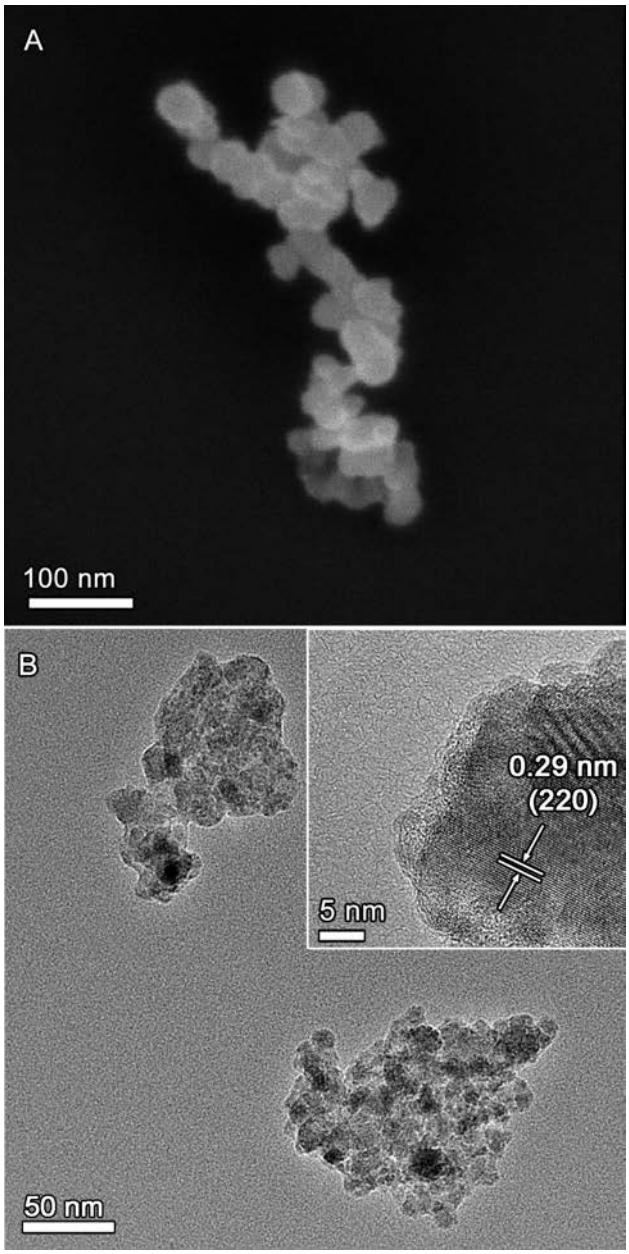

Figure 4. (A) SEM and, (B) TEM images of γ Fe_2O_3/SiO_2 particles. The inset in (B) shows the HRTEM image the edge of a single γ Fe_2O_3/SiO_2 particle.

Figure 6, A–C, show pictures of γ-Fe_2O_3@[$Eu(TTA)_3$(Bpy-Si)] suspension under white light, UV light and UV light with additional external magnet field. In contrast with the brownish color of the suspension observed under white light, an intense red color is homogenously seen under UV light exposure for γ-Fe_2O_3@[$Eu(TTA)_3$(Bpy-Si)]. After few minutes that an external magnetic field is approached from a particular wall of the cuvette, a layer of γ-Fe_2O_3@[$Eu(TTA)_3$(Bpy-Si)] particles is formed also displaying a red color under UV light. Therefore, the γ-Fe_2O_3@[$Eu(TTA)_3$(Bpy-Si)] nanocomposite can quickly respond to the external magnetic field and quickly redisperse once the external magnetic field is removed.

Figure 6, D and E, gather the excitation and emission spectra for powdered [$Eu(TTA)_3$(Bpy-Si)] complex and γ-Fe_2O_3@[$Eu(TTA)_3$(Bpy-Si)] at room temperature. It is worth to pointing out that no detectable photodegradation was noticed during luminescence measurements. The excitation spectra were recorded with emission monitored at 610 nm. From Figure 6D, broad bands observed in the ultraviolet region for both pure and grafted silylated Eu complex refer to ligand-to-metal energy transfer (antenna effect). The band at 277 nm is assigned to π - π* transitions from bipyridine rings of silylated Eu complex. The band centered at 340 nm with a shoulder at 366 nm observed for γ-Fe_2O_3[$Eu(TTA)_3$(Bpy-Si)] is attributed π - π* transitions of TTA ligand. This band is red-shifted for pure silylated Eu complex being encountered at 367 nm.[27] As previously reported, the effect of the concentration of luminescent species also causes distortions on the shape of the excitation bands of powdered [$Eu(TTA)_3$(Bpy-Si)] complex compared to that of the silylated Eu complex grafted on silica surface of nanoparticles because, in the latter case, the luminescent species are diluted. Nevertheless, the narrow bands at 463 and 533 nm assigned to $^7F_{0,1} \rightarrow {}^5D_2$ and $^7F_1 \rightarrow {}^5D_2$ transitions of Eu^{3+}, respectively, were only noticeable in the excitation spectrum of pure Eu silylated complex also due to effect of the concentration of the luminescent specie on the powdered sample.

The emission spectra of pure silylated complex and γ-Fe_2O_3@[$Eu(TTA)_3$(Bpy-Si)] particles are shown in Figure 6E. Both spectra show characteristic peaks of intra-4f^6 narrow bands of Eu^{3+} ($^5D_0 \rightarrow {}^7F_{J\ 0\text{-}4}$) transitions. The following emission lines are seen: $^5D_0 \rightarrow {}^7F_0$ (576.2 nm), $^5D_0 \rightarrow {}^7F_1$ (587.4 and 592.4 nm), $^5D_0 \rightarrow {}^7F_2$ (608.2, 613.5 and 620.9 nm), $^5D_0 \rightarrow {}^7F_3$ (647.8 nm), $^5D_0 \rightarrow {}^7F_4$ (687.9 and 700 nm). The strongly forbidden transition $^5D_0 \rightarrow {}^7F_0$ presents only one line, which is consistent with only one site

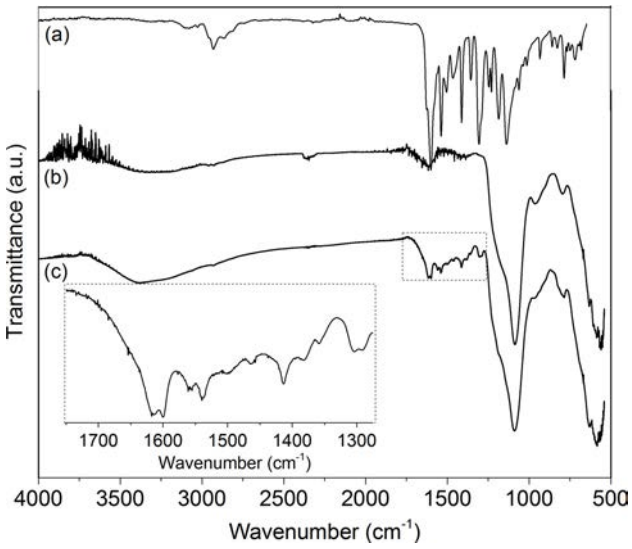

Figure 5. ATR FTIR of (a) Pure [Eu(TTA)$_3$(Bpy Si)], (b) γ Fe_2O_3/SiO_2 and, (c) γ Fe_2O_3@[Eu(TTA)3(Bpy Si)]. The inset shows the amplified 1780 1260 cm 1 region of γ Fe2O3@[Eu(TTA)$_3$(Bpy Si)] displaying the vibrational modes of silylated Eu complex grafted on γ Fe_2O_3/SiO_2.

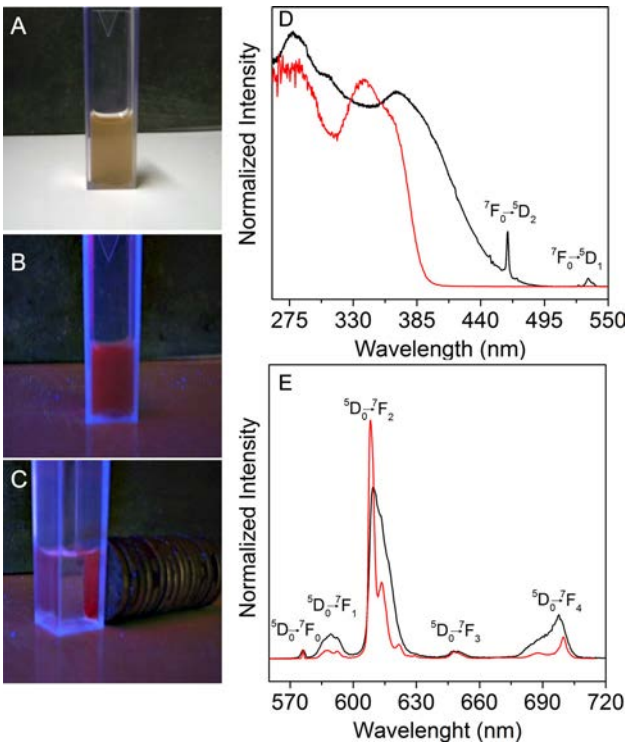

Figure 6. Pictures of an ethanolic suspension of γ Fe_2O_3@[Eu(TTA)$_3$(Bpy Si)] under (A) white light, (B) UV light with $\lambda_{max} = 365$ nm, and (C) under UV light and external magnetic field. (D) Excitation spectra monitoring 610 nm and (E) emission spectra by excitation at 360 nm of pure [Eu(TTA)$_3$(Bpy Si)] complex and γ Fe_2O_3@[Eu(TTA)$_3$(Bpy Si)] particles.

being occupied by the Eu^{III} ion. The full width at half maximum value of this band is larger than 30 cm ^{1} implying that Eu^{III} ions have small energy distribution and should have a low-symmetry coordination environment (polymeric nature). The forced electric dipole transition band at 608 nm, $^5D_0 \rightarrow {}^7F_2$ is the most intense band in the emission spectra of both pure [Eu(TTA)$_3$(Bpy-Si)] complex and γ-Fe_2O_3@[Eu(TTA)$_3$(Bpy-Si)] particles indicating that Eu^{III} lie at low symmetry site. Interestingly, this transition is relatively higher for γ-Fe_2O_3@[Eu(TTA)$_3$(Bpy-Si)] comparing to the pure Eu complex while the $^5D_0 \rightarrow {}^7F_{1,4}$ transitions display lower intensities. The larger inhomogeneous broadening observed for $^5D_0 \rightarrow {}^7F_0$ transition in the γ-Fe_2O_3@[Eu(TTA)$_3$(Bpy-Si)] particles is compatible with a more wide distribution of slightly different chemical environment.

The lifetimes (τ, in ms) of the emitting level, $^5D_0$ were measured by excitation at 360 nm and monitoring at 610 nm. The luminescence decay curve, with emission monitored at $^5D_0 \rightarrow {}^7F_2$, was fitted by a single exponential decay function as displayed in Figure 7. We observe a significant decrease in the

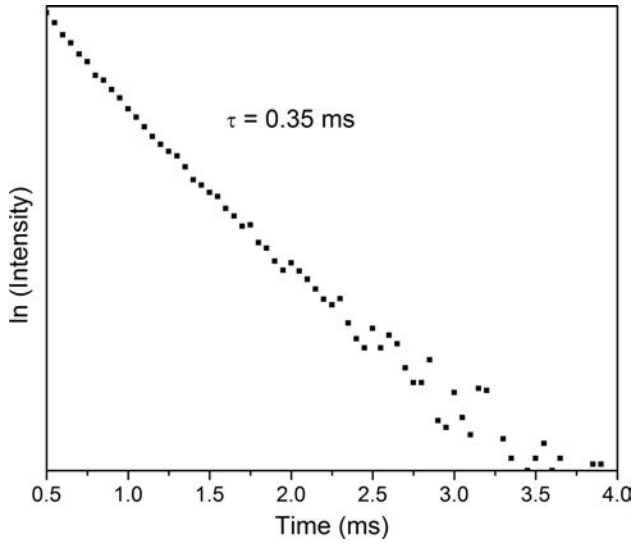

Figure 7. Luminescence decay curves, at room temperature, of the $^5D_0$ emitting level of powdered γ Fe_2O_3@[Eu(TTA)$_3$ (Bpy Si)] particles by excitation at 360 nm and monitored at 610 nm. The estimated lifetime was 0.35 ms by fitting a decay curve.

lifetime for γ-Fe_2O_3@[Eu(TTA)$_3$(Bpy-Si)] comparing to pure silylated Eu complex: (i) 0.35 ms for silylated Eu complex and γ-Fe_2O_3@[Eu(TTA)$_3$(Bpy-Si)] (ii) 0.60 ms for [Eu)(TTA)$_3$(Bpy-Si)] as reported by Duarte et al.[26] Such difference may arise due to the presence of defects on the surface of γ-Fe_2O_3 particles. As such, the defects may cause the anchorage of silylated Eu complex susceptible to undergo significant dissociation of weakly coordinated ligands, thereby losing the original optical properties comparing to pure silylated Eu complex.

From the magnetization curve shown in Figure 8 A, it was found that the saturation magnetization (MS) value of of pristine γ-Fe_2O_3 is 60 emu.g ^{1}. The hysteresis loops display a typical profile of superparamagnetism phenomenon. Notwithstanding, the magnetization curve of silica coated γ-Fe_2O_3 nanoparticles did not cause any significant change on the profile of magnetization curves which is featured by small

coercivity (< 38 Oe) at room temperature as shown in Figure 8B. After the grafting of silylated Eu complex, the MS value decreases to 0.12 emu.g ^{1} and the remanent magnetic field increases to 37 Oe at room temperature as shown in Figure 8C. The decrease of MS after functionalization could arise from the increase of nonmagnetic content surrounding the γ-Fe_2O_3 nanoparticles with the functionalization of silylated Eu complex as also reported in the literature.[17,22,23]

Conclusions

In summary, we have fabricated bi-functional γ-Fe_2O_3@[$Eu(TTA)_3$ (Bpy-Si)] nanoparticles with conceiving coated magnetic cores with thin silica layer and covalently grafted by luminescent europium complex possessing a silylil functional group. Magnetic measurements showed that the obtained nanocomposites exhibited superparamagnetic behavior. In addition, emission spectra indicated that the nanocomposite exhibited high red luminescence intensity under UV exposition with lifetime in the milliseconds range, which enables, for example, temporal discrimination of optical signal from background fluorescence displayed by biological tissues. Therefore, the new bifunctional nanocomposite could be detected by feasible conventional optical means and be manipulated by an external magnetic field extending its potential applications to a myriad of bioanalytical assays.

Acknowledgements

The authors are grateful to the financial support from the Brazilian agencies: Coordenação de Pessoal de Ensino Superior (CAPES) and Conselho Nacional de Desenvolvimento Científico e Tecnológico (CNPq). We also acknowledge the National Laboratory of Nanotechnology (LME/LNNano/CNPEM) for the technical support during the electron microscopy data collection. R. R. Silva thanks to the Fundação de Amparo à Pesquisa do Estado de São Paulo (FAPESP) for the Grant No. 2013/12367-6

Keywords: β-diketone · luminescent · maghemite · silylated · superparamagnetic

[1] N. Lee, D. Yoo, D. Ling, M. H. Cho, T. Hyeon, J. Cheon, *Chem. Rev.* **2015**, *115*, 10637 10689.
[2] T. H. Shin, Y. Choi, S. Kim, J. Cheon, *Chem. Soc. Rev.* **2015**, *44*, 4501 4516.
[3] L. D. Carlos, R. S. Ferreira, V. D. Z. Bermudez, S. J. L. Ribeiro, *Adv. Mater.* **2009**, *21*, 509 534.
[4] J. C. G. Bünzli, *J. Lumin.* **2016**, *170*, 866 878.
[5] J. G. Bünzli, *Coord. Chem. Rev.* **2015**, *293 294*, 19 47.
[6] S. V. Eliseeva, J. C. G. Bünzli, *Chem. Soc. Rev.* **2010**, *39*, 189 227.
[7] X. Li, D. Zhao, F. Zhang, *Theranostics* **2013**, *3*, 292 305.
[8] L. U. Khan, H. F. Brito, J. Hölsä, K. R. Pirota, D. Muraca, M. C. F. C. Felinto, E. E. S. Teotonio, O. L. Malta, *Inorg. Chem.* **2014**, *53*, 12902 12910.
[9] D. Tu, Y. Liu, H. Zhu, X. Chen, *Chem. A Eur. J.* **2013**, *19*, 5516 5527.
[10] Y. Zhang, S. Pan, X. Teng, Y. Luo, G. Li, *J. Phys. Chem. C* **2008**, *112*, 9623 9626.
[11] F. Chen, W. Bu, L. Zhang, Y. Fan, J. Shi, *J. Mater. Chem.* **2011**, *21*, 7990.
[12] C. Mi, J. Zhang, H. Gao, X. Wu, M. Wang, Y. Wu, Y. Di, Z. Xu, C. Mao, S. Xu, *Nanoscale* **2010**, *2*, 1141.
[13] Z. Liu, G. Yi, H. Zhang, J. Ding, Y. Zhang, J. Xue, *Chem. Commun.* **2008**, *1*, 694 696.
[14] M. Guglielmi, G. Kickelbick, A. Martucci, *Sol Gel Nanocomposites*, Springer New York, New York, NY, **2014**.
[15] C. D. S. Brites, P. P. Lima, N. J. O. Silva, A. Millán, V. S. Amaral, F. Palacio, L. D. Carlos, *Adv. Mater.* **2010**, *22*, 4499 4504.
[16] C. D. S. Brites, P. P. Lima, N. J. O. Silva, A. Millán, V. S. Amaral, F. Palacio, L. D. Carlos, *J. Lumin.* **2013**, *133*, 230 232.
[17] P. Lu, J. L. Zhang, Y. L. Liu, D. H. Sun, G. X. Liu, G. Y. Hong, J. Z. Ni, *Talanta* **2010**, *82*, 450 457.
[18] M. N. Luwang, S. Chandra, D. Bahadur, S. K. Srivastava, *J. Mater. Chem.* **2012**, *22*, 3395.
[19] Y. J. Zhu, W. W. Wang, R. J. Qi, X. L. Hu, *Angew. Chemie* **2004**, *116*, 1434 1438.
[20] B. Wang, J. Hai, Q. Wang, T. Li, Z. Yang, *Angew. Chemie* **2011**, *50*, 3063 3066.
[21] S. Y. Yu, H. J. Zhang, J. B. Yu, C. Wang, L. N. Sun, W. D. Shi, *Langmuir* **2007**, *23*, 7836 7840.
[22] J. Feng, W. Q. Fan, S. Y. Song, Y. N. Yu, R. P. Deng, H. J. Zhang, *Dalt. Trans.* **2010**, *39*, 5166.
[23] J. Feng, S. Y. Song, R. P. Deng, W. Q. Fan, H. J. Zhang, *Langmuir* **2010**, *26*, 3596 3600.
[24] S. Cousinié, M. Gressier, P. Alphonse, M. Menu, *Chem. Mater.* **2007**, *19*, 6492 6503.
[25] S. Cousinié, M. Gressier, C. Reber, J. Dexpert Ghys, M. J. Menu, *Langmuir* **2008**, *24*, 6208 6214.
[26] A. P. Duarte, M. Gressier, M. J. Menu, J. Dexpert Ghys, J. M. A. Caiut, S. J. L. Ribeiro, *J. Phys. Chem. C* **2012**, *116*, 505 515.
[27] A. P. Duarte, L. Mauline, M. Gressier, J. Dexpert Ghys, C. Roques, J. M. A. Caiut, E. Deffune, D. C. G. Maia, I. Z. Carlos, A. A. P. Ferreira, S. J. L. Ribeiro, M. J. Menu, *Langmuir* **2013**, *29*, 5878 5888.

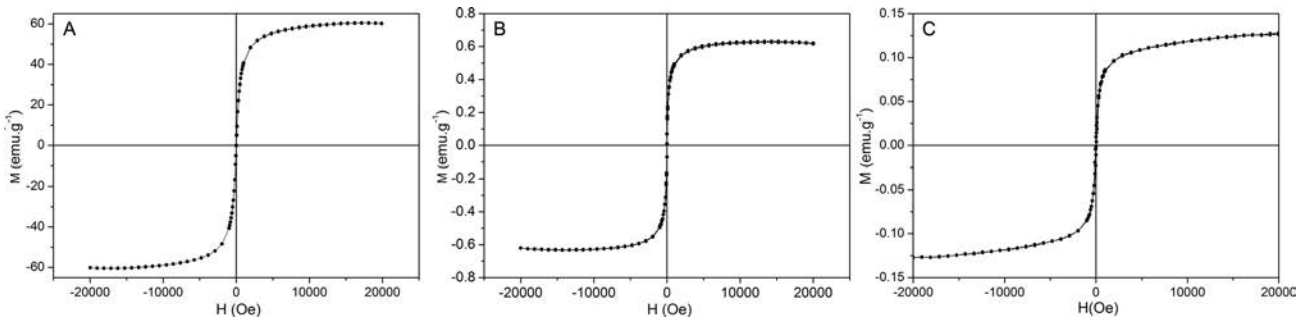

Figure 8. Magnetization curve of (A) pristine γ Fe_2O_3 nanoparticles and (B) γ Fe_2O_3/SiO_2 particles, and (C) γ Fe_2O_3@[$Eu(TTA)_3$(Bpy Si)] particles.